Chemical constituents, physical, and mechanical properties of Indonesian sugar palm (*Arenga longipes* Mogea) trunk

*Luthfi Hakim**
Assoc. Professor
Lab. of Forest Product Technology, Faculty of Forestry, Universitas Sumatera Utara
Deli Serdang, 20353
E-mail: luthfi@usu.ac.id

Ganis Lukmandaru
Professor
Faculty of Forestry, Universitas Gadjah Mada
Yogyakarta, 55281
Email: glukmandaru@ugm.ac.id

Jajang Sutiawan
Senior researcher
Research Center for Biomass and Bioproduct, National Research and Innovation Agency
Cibinong, 16911
Email: Jajang.sutiawan@brin.go.id

Tito Sucipto
Assistant Professor
Lab. of Forest Product Technology, Faculty of Forestry, Universitas Sumatera Utara
Deli Serdang, 20353
Email: tito@usu.ac.id

Apri Heri Iswanto
Professor
Lab. of Forest Product Technology, Faculty of Forestry, Universitas Sumatera Utara
Deli Serdang, 20353
Email: apri@usu.ac.id

Yunida Syariani Lubis
Junior researcher
Research Center for Applied Botany, National Research and Innovation Agency
Cibinong, 16911
Email: yuni030@brin.go.id

Erlina Nurul Aini
Junior researcher
Research Center for Biomass and Bioproduct, National Research and Innovation Agency
Cibinong, 16911
Email: erli010@brin.go.id

(Received 24 October 2024)

Abstract. Wood density, chemical characteristics, and mechanical properties in the stem (vertical and horizontal) were studied for the Indonesian sugar palm (*Arenga longipes*) grown in Sumatera Island in Indonesia. This species is widely used industrially and is widely distributed on the island of North Sumatra. A 15-year-old palm tree was harvested (40 cm diameter at breast height) then sampled at seven heights above the ground (1, 2, 3, 4, 5, 6, and 7 m of trunk height) and at five horizontal positions (4, 8, 12, 16, and 20 cm of radius from the bark) at each height. The sections were evaluated for chemical constituents, density, modulus of rupture (MOR), modulus of elasticity (MOE), tensile strength, and compression strength using British Standard BS 373 (1957). The chemistry of the trunk was also evaluated by gas chromatography-mass spectroscopy (GC-MS), Fourier transform-infrared spectroscopy (FTIR), and thermogravimetric analysis (TGA). The distribution of chemical constituents of *A. longipes* stem was as follows: 24.97–39.23% α-cellulose, 68.03–78.04% holocellulose, 23.01–34.44% lignin, and 1.62–3.41% ash content. Density varied from 0.13 to 0.75 g/cm^3. Modulus of rupture varied from 10.42 to 143.49 MPa, modulus of elasticity varied from 0.35 to 24.92 GPa, tensile strength ranged from 0.55 to 16.03 GPa, and compressive strength ranged from 0.53 to 6.14 MPa. Hexadecenoic acid and octadecanoic acid were both detected, and the latter compound was most common (97.98% of peak area). The FTIR analysis indicated a hydrophilic tendency in the material, which was attributed to the presence of hydroxyl functional groups in cellulose and lignin. Thermal decomposition occurred at temperatures as high as 402°C, representing an 18% degradation. The horizontal variation within the trunk was highly significant for all traits, while the vertical variation was significant only for density and mechanical properties. A strong correlation was observed between density and mechanical properties. *A. longipes* has potential as an alternative raw material, capable of supplying the industry with valuable timber substitutes, particularly for material from the outer circumference of the stem.

Keywords: Chemical properties, Density, Modulus of rupture, Sugar palm, Horizontal variability, Vertical variability

* Corresponding author

Introduction

Arenga, a genus of palms native to Asia, is renowned for producing edible products from both its sap and fruit (Johnson 1992). The Indonesian sugar palm, *Arenga longipes*, was first identified on Sumatra Island by Mogea (2004), and it has since been recognized as a multi-purpose plant, classified as a non-timber forest product (NTFP). On Sumatra, particularly in North Sumatra, *A. longipes* has long been cultivated by local communities, primarily for tapping its sap to produce palm sugar and traditional wine (Azhar et al. 2019; Fadhilla et al. 2023). The fruit of *A. longipes* is also rich in carbohydrates and has been used as a traditional food source (Gunawan et al. 2018). Despite its extensive use in Indonesia, *A. longipes* has not been widely explored or utilized in India, particularly with regard to its stem (Pillai et al. 2020). In contrast, another species of sugar palm (*A. pinnata*) is an integral part of local economies in Malaysia, where it is utilized for producing palm sugar and the fruit known as "*kolang-kaling*" (Muda et al. 2024).

Historically, the sugar palm has been cultivated in Indonesia through agroforestry systems and is classified as a multi-purpose tree species (MPTS), providing various livelihood benefits to local communities (Haryoso et al. 2020; Mogea et al. 1991). In 2020, the area under sugar palm cultivation in North Sumatra was estimated at 7,063 hectares, yielding 6,619 tons of palm sugar (BPS 2021). These community-managed plantations are often subject to selective cutting for traditional building materials and flooring, and the trunks have considerable market value for the production of wood-based products (Nuryawan et al. 2017). However, despite its growing importance, little is known about the lignocellulosic properties of *A. longipes* trunks, with most studies focusing on plant morphology (Nirawati et al. 2020) and the diversity of its uses, tapping flow discharge, and conservation efforts (Fadhilla et al. 2023). Our previous research has examined the anatomical, fiber morphology, and mechanical properties of *A. longipes* fronds (Hakim et al. 2023); and properties for construction applications, such as density and mechanical strength (modulus of rupture – MOR; modulus of elasticity – MOE), are also of particular interest. These properties are often correlated with density, which influences the performance and quality of the final products (Hakim et al. 2022).

Previous studies on *A. pinnata* have suggested that its trunk could serve as a raw material for wood substitutes, suggesting the potential for similar applications with *A. longipes* due to the morphological similarities between the two species. The trunk of *A. longipes* is particularly notable for its fibrous, spongy texture, which is both strong and lightweight. Its structure consists of thick, interwoven fibers, providing high mechanical strength and flexibility, making it useful for applications such as construction, handicrafts, and furniture production.

The overall objective of this study was to assess the chemical, physical, and mechanical properties of Indonesian sugar palm (*A. longipes*) in Indonesia as a high-value wood substitute.

Materials and Methods

Sample preparations

A 15-year-old *A. longipes* trunk was harvested from Langkat district, North Sumatra Province, Indonesia (Figure 1) at the end of production for tapping sap. The trunk had a 40-cm over bark diameter at breast height. Diameter at 1.3 m height (diameter at breast height) was determined as the mean of two cross diameters, and the stem was trimmed to 7 m. Forty-centimeter-thick disks were cut at 1, 2, 3, 4, 5, 6, and 7 m of total trunk height. Specimens were cut at five distances from the bark to the pith / horizontal direction (4, 8, 12, 16, and 20 cm of the radius length). All vertical and horizontal treatments were repeated five times. The complete sampling and repetition techniques are shown in Table 1. The specimens were conditioned to constant mass at 25 ± 2 °C and 65% ± 5% relative humidity and maintained in this condition until required for testing. The average moisture content of the test pieces after this stage was 12%. Figure 2 is an illustration of sample pattern in both vertical and horizontal directions.

Chemical constituents, physical and mechanical testing

Holocellulose, α-cellulose, lignin content, and ash were evaluated on 25 specimens per radial stem position. Holocellulose content was analyzed based on ASTM D 1104 (1978), using 40-50 mesh extractive-free powder (pre-extracted using ethanol-toluene). As much as 0.7 ± 0.05 g (*W1*) of oven-dried powder was put into 50 mL acetic acid and 2% NaOH. One L

Table 1. Experimental plan used to assess the properties of *A. longipes* stems

Vertical direction	Horizontal direction				
	4 cm	8 cm	12 cm	16 cm	20 cm
1 m	V_1H_1	V_1H_2	V_1H_3	V_1H_4	V_1H_5
2 m	V_2H_1	V_2H_2	V_2H_3	V_2H_4	V_2H_5
3 m	V_3H_1	V_3H_2	V_3H_3	V_3H_4	V_3H_5
4 m	V_4H_1	V_4H_2	V_4H_3	V_4H_4	V_4H_5
5 m	V_5H_1	V_5H_2	V_5H_3	V_5H_4	V_5H_5
6 m	V_6H_1	V_6H_2	V_6H_3	V_6H_4	V_6H_5
7 m	V_7H_1	V_7H_2	V_7H_3	V_7H_4	V_7H_5

Note: each sample was repeated five times.

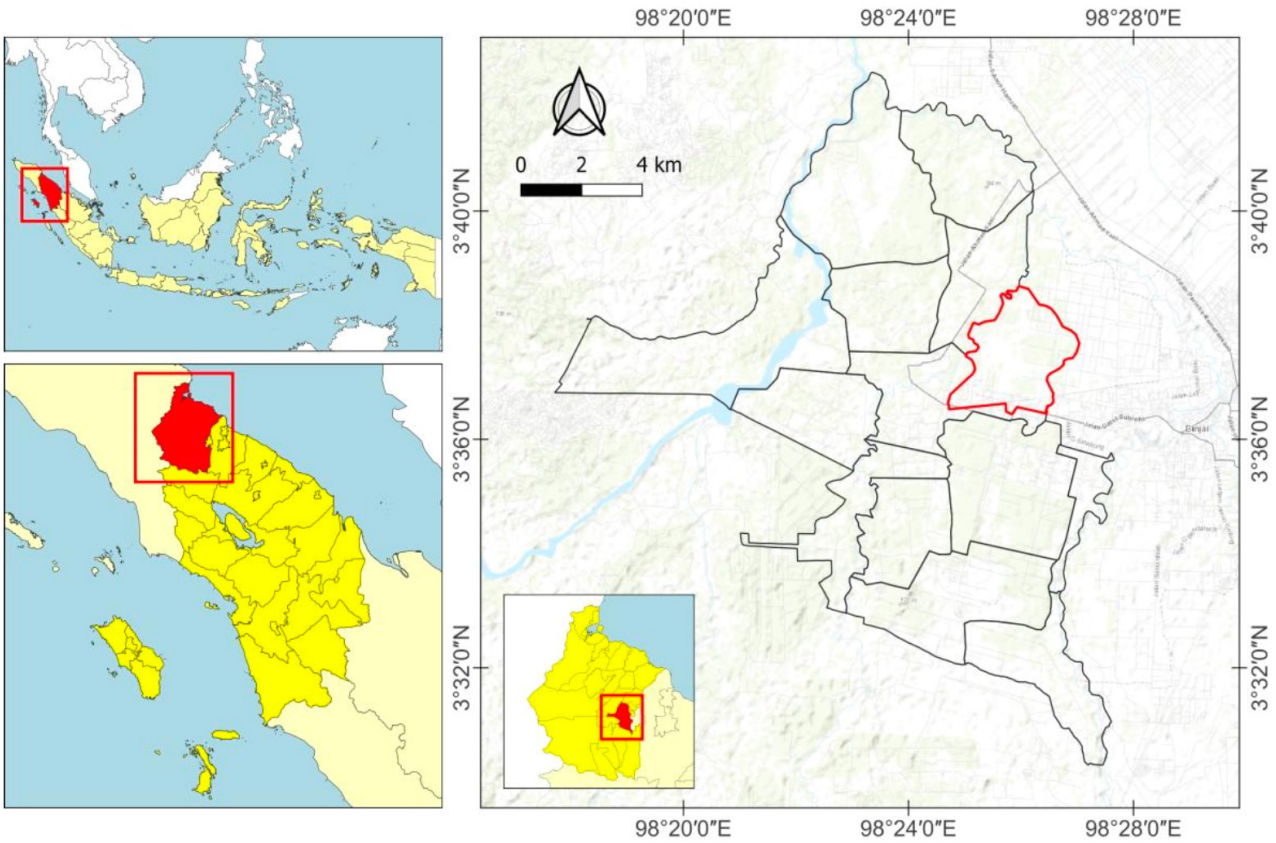

Figure 1. Location of *A. longipes* harvesting in Langkat district, North Sumatera, Indonesia.

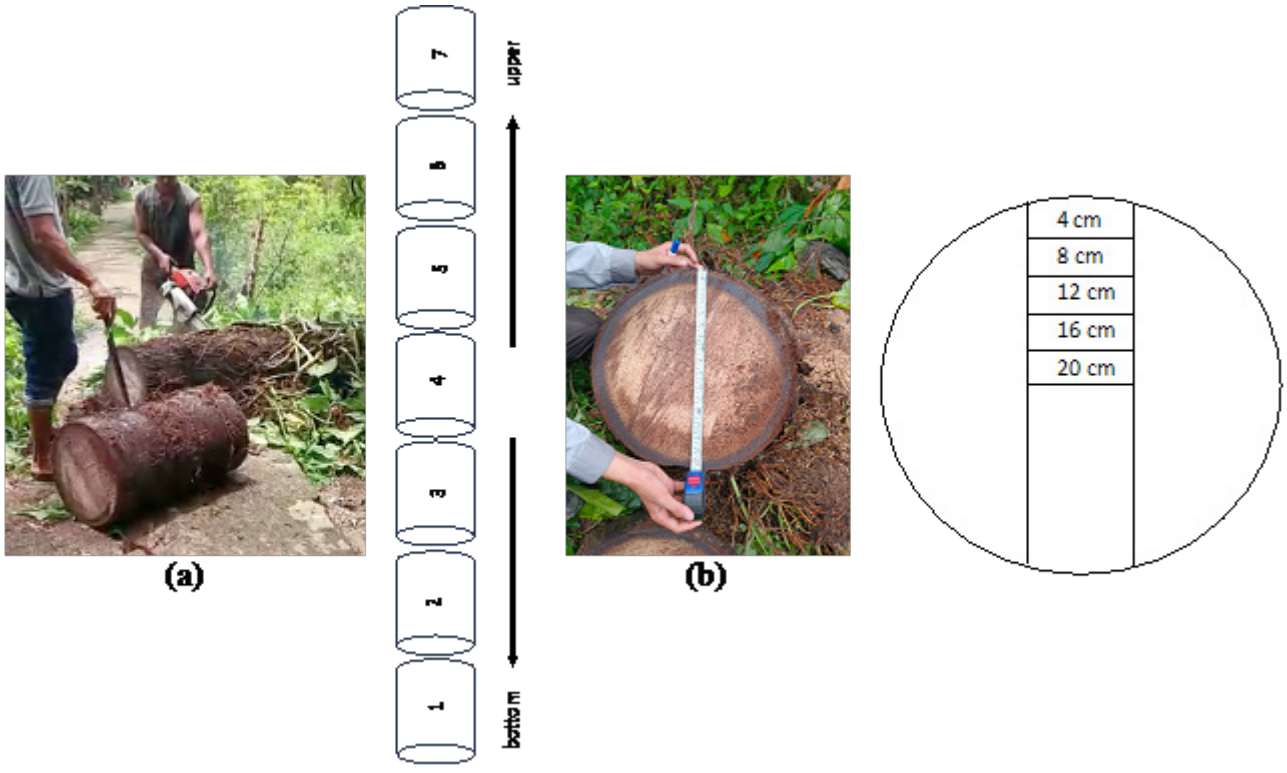

Figure 2. Photograph and schematic showing (a) vertical directions and (b) horizontal directions on the *A. longipes* stems.

of 20% $NaClO_2$ (w/v) solution was added and heated at 70°C while shaking every 30 minutes for 150 minutes. One ml of 20% $NaClO_2$ was added after 45, 90, and 150 minutes. The solution was heated for 4 hours, then cooled in ice water, and 15 mL of distilled water was added. The sample was filtered and washed successively with 100 ml of 1% acetic acid and 2–5 mL of acetone, then oven dried to constant mass at 103 ± 2 °C (*W2*) and weighed. Holocellulose content was calculated based on the equation below:

$$\text{Holocellulose (\%)} = \frac{W2}{W1} x100\% \quad (1)$$

Cellulose content was determined according to ASTM D 1103 (2001). The powder prepared for holocellulose analysis was used to determine α-cellulose content. The holocellulose was dissolved in 3 ml of 17.5% NaOH until completely submerged, and the mixture was stirred for 1 minute (*W1*). After soaking for 5 minutes, 3 ml of 17.5% NaOH was added and the mixture was stirred again for + 1 minute. The solution was left for 35 minutes, then 6 mL of distilled water was added before the mixture was filtered and washed with 60 mL of distilled water. Ten mL of 10% acetic acid was added with stirring. The mixture was filtered and washed with 60 mL of distilled water and 10 mL of acetone. The sample was oven dried to constant mass at 103 ± 2 °C and weighed (*W2*). The α-cellulose content was calculated based on the equation below:

$$\alpha\text{-cellulose (\%)} = \frac{W2}{W1} x100\% \quad (2)$$

Lignin content was determined based on ASTM D 1106 (2021). Up to 1 g (*W1*) of extractive-free powder was dissolved in 400 mL of boiling water and heated for 3 hours. The material was filtered and air-dried then dissolved in 15 mL of 72% sulfuric acid at 12–15°C for 1 minute. The mixture was left for 2 hours at 18–20°C with occasional stirring. The sample was heated in boiling water for 4 hours. Insoluble materials that precipitated were removed by filtration, and the filtrate was washed with hot water to remove residual acid. The samples were oven dried to constant mass at 103 ± 2 °C (*W2*). Lignin content was calculated based on the equation below:

$$\text{Lignin content (\%)} = \frac{W2}{W1} x100\% \quad (3)$$

Ash content was determined according to the ASTM D 1102 (2021). Around 2 g of sugar palm stem ground to 40-60 mesh (*W1*) was put into a furnace and heated at 600°C for 1 hour, cooled in a desiccator, and oven dried to constant mass at 103 ± 2 °C (*W2*). Ash content was calculated by the equation below:

$$\text{Ash content (\%)} = \frac{W2}{W1} x100\% \quad (4)$$

Mass and volume were measured after 2-cm cubes from each location were conditioned to 12% moisture content. Samples were measured before and after conditioning to determine shrinkage. The tests were performed on 25 specimens per radial stem position. Density was calculated by the equation below:

$$\text{Density (g/cm}^3\text{)} = \frac{Wood\ mass\ (g)}{Wood\ Volume\ (cm^3)} \quad (5)$$

The mechanical testing consisted of MOR, MOE, tensile strength, and compression tests. The mechanical tests were performed on 25 specimens per radial stem positions. The MOR and MOE were determined by a three-point bending test according to British Standard BS-373 (1957) on 2-cm by 2-cm by 30-cm-long beams with a 28-cm span. Load was applied at a rate of 6.5 mm/min. Load and displacement were continuously measured to failure, with a 1% deformation accuracy. A total of 25 specimens were tested per radial stem position.

Tension and compression parallel to grain strength were determined according to British Standard BS-373 (1957). For tensile tests, the form and dimensions of the test piece used in one method to determine tension parallel to grain strength must be as shown in the British Standard (1957). The test piece was positioned so that the direction of the annual rings in the cuboidal section was perpendicular to the bigger cross-sectional dimensions. The actual dimensions of the minimum cross-section must be measured. Load was applied at a constant head speed. Compression and tension load were applied to the test piece at a constant head speed of 1.25 mm per minute to failure. Tensile strength was calculated as the load/cross sectional area. Compression and tension tests were performed on a 50 kN universal testing machine (Tensilon RTF 1350, Japan) A total of 25 samples were tested for compression or tension at each position in the trunk.

Gas chromatography-mass spectroscopy analysis

Sugar palm trunk powder was extracted in an ethanol and benzene solution (1:0.4 v/v) for 8 hours. The extractive solution was analyzed using gas chromatography-mass spectrometry (GC-MS) on an Agilent Technologist, Mass Hunter 5977 (GC-MS 7890B, Santa Clara, CA USA) and a mass detector. The carrier gas utilized was helium with a flow rate of 1 mL per minute. One µL of the supernatant was injected into the GC-MS. Temperature was raised at a rate of 15°C per minute from 80°C to 200°C, then at 5°C per minute from 200°C to 280°C, and held at a constant temperature of 280°C for 5 minutes. The ion source was set at 230°C, and an ionization

potential of 70 eV was selected. The GC-MS interpretation relied on the National Institute of Standards and Technology (NIST) database (Lovestead and Urness 2019).

Fourier transform infrared (FT-IR) analysis

Sugar palm trunk powder samples were boiled for 2 hours to remove any extractives. After cooling the samples were stored for 1 hour at room temperature. The samples were filtered through a 100-mesh screen and the precipitate was dried for 12 hours at 35 ± 5 °C. The samples were mixed with KBr and compressed to a pellet that was analyzed on a Shimadzu FTIR-4200 spectrophotometer (Shimadzu, Tokyo, Japan) at a resolution of 12 cm^{-1}. Peaks were subjected to auto-correction and assigned to certain functional groups.

Thermogravinetry analysis (TGA)

Thermal stability and rate of mass change of the sugar palm trunk were measured by thermogravimetric analysis using an Ekstar SIII-Type 7300 Thermogravimetric Analyser (Hitachi, Tokyo, Japan). Approximately 10 mg were heated in an aluminum crucible from room temperature, gradually increasing to 600°C at a rate of 10°C per minute under a nitrogen at a flow rate of 30 mL/min.

Data analysis

The experimental design was a factorial complete randomized design with vertical and horizontal direction as factors. An analysis of variance (ANOVA) was performed according to the linear model. Variance components for the sources of variation were also estimated. Differences between means were examined using Duncan's multiple range test at $\alpha = 0.05$. Correlation coefficients between density and mechanical properties were calculated by considering the average values per sample by linear regression analysis using the least squares method. Statistical analysis was performed using R-studio version 4.2.2.

Results and discussion

Chemical content

Figure 3 shows the α-cellulose, holocellulose, lignin, and ash content of the *A. longipes* stem. Generally, α-cellulose content decreased from bark to the pith (horizontally) with a higher value of 39.23% at the bottom and outer position to a lower value of 24.97% at the upper and inner position. The α-cellulose content did not differ significantly from the bottom to the upper position, although there was a general decrease;

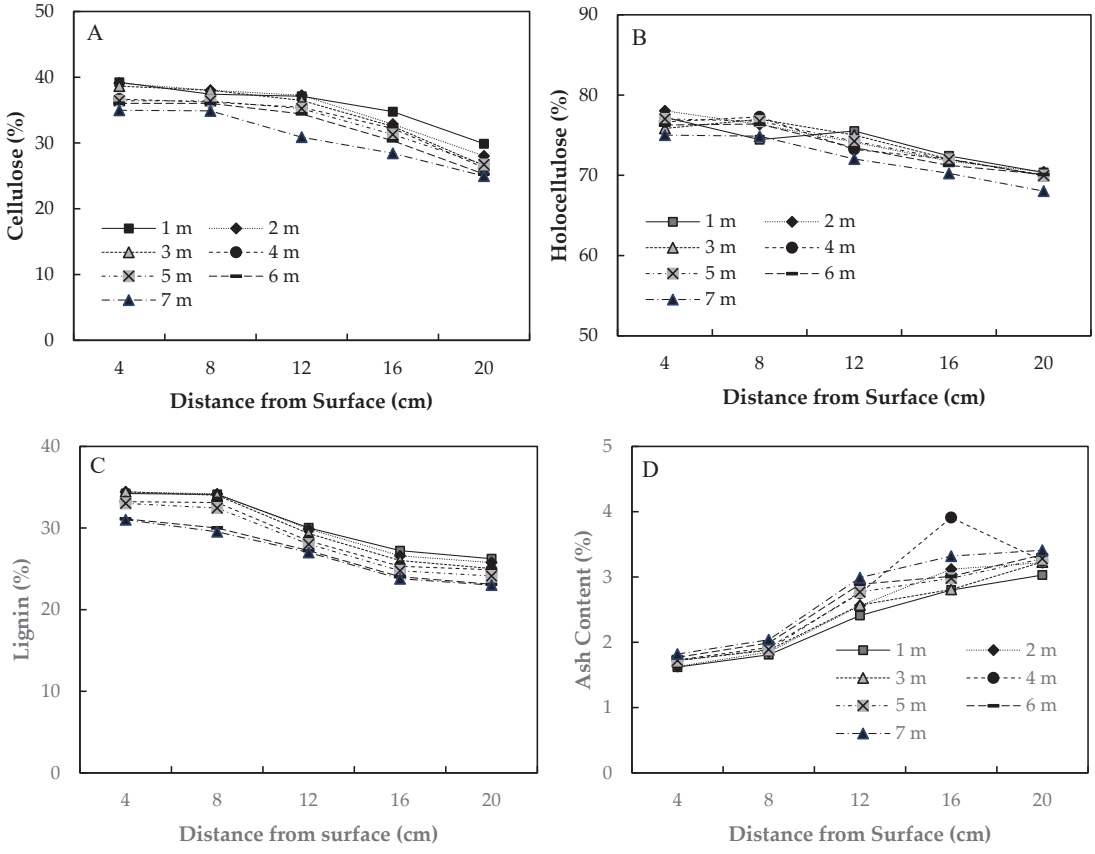

Figure 3. Concentrations (% m/m) of cellulose, holocellulose, lignin, and ash at selected distances above the ground and inward from the bark of an *A. longipes* stem.

α-cellulose content near the bark tended to be higher than towards the pith. This phenomenon likely reflects the higher density in that zone, reflecting the need to concentrate flexural properties around the circumference. Figure 1 (a) shows that the peripheral zone was only 2–3 cm thick, while the stem diameter was 40 cm. In addition, the density of palm wood is affected by the abundance of fibrovascular bundle (FVB) tissue. Conversely, increased parenchyma tissue towards the pith has less cellulose. Sahari et al. (2012) reported that *A. pinnata* contained 40.6% α-cellulose in the trunk which was slightly higher than that of *A. longipes*. Cellulose content of palm trees increases with increasing height; however, as the palm trees get older, the content decreases, which has been related to the maturity stage of the fiber (Imraan et al. 2023).

Trends with holocellulose content were similar to those for α-cellulose. Holocellulose content tended to decrease from the bark to the pith, reflecting the important of cellulose in the outer circumference supporting the stem. There was no significant difference in holocellulose content with distance from the ground, although levels were slightly higher near the base. Holocellulose content in *A. longipes* tended to decrease from the bottom to the upper position, as well as the outer (periphery) to the pith. The high carbohydrate content in *A. longipes* reflects the fact that this palm can produce a lot of sugar. A previous study of *A. pinnata* found holocellulose contents of 61.1%, 81.2%, 71.8%, and 65.6% for sugar palm trunk, frond, sugar palm bunch, and black fiber, respectively (Wulandari and Erwinsyah 2020).

Lignin distribution along the trunk also tended to decrease from the bottom to the top and from the periphery to the pith and ranged from 34.44% to 23.01%. Our previously research reported that the lignin content of the *A. longipes* bunch was 27.23%, which is lower than that of the trunk (Hakim et al. 2024). Sahari et al. (2012) reported that the lignin content of the *A. pinnata* trunk was higher at 46.4%,

Ash content tended to increase from the periphery to the pith (horizontal), but was similar with height. Ash content of *A. longipes* was slightly lower than *A. pinnata* actively (Sahari et al. 2012).

Wood density of *A. longipes trunk*

Air-dry density (at 12% moisture content) of the Indonesian sugar palm trunk ranged from 0.13 to 0.75 g/cm^3 (Table 2). Density was significantly higher at the bottom and outer section of the trunk. Density 1 m from the base had the largest range, with mean values from 0.73 to 0.75 g/cm^3. Density also decreased significantly from the bark (4 cm) to the pith (16 cm), then remained constant further inward. Density variations in palms reflect the presence of FVB tissue (fiber, xylem, and phloem) whose frequency tends to decrease from the skin towards the pith (Hakim et al. 2021; Srivaro et al. 2018a; Takoumbe et al. 2023; Wulandari and Erwinsyah 2020). Lower density in the middle zone of the stem is affected by the large amount of parenchyma tissue, which does not have a structural function in supporting the stem and tends to be less dense (Srivaro et al. 2020). These results were similar to those found for coconut palm wood and oil palm trunk zones (Rana et al. 2015; Srivaro et al. 2018b). Rana et al. (2015) also reported that coconut palm wood was denser in the core than the peripheral zone.

Hartono et al. (2019) found that *A. pinnata* had a significantly lower density (0.12–0.51 g/cm^3) at the same age (15 years) than *A longipes*. Another palm (*Elaeis guenensis*) had a density range of 2.22–4.04 g/cm^3, also lower than the density of *A. longipes* (Srivaro et al. 2018a). Likewise, the density of coconut (*Cocos nucifera*) trunk is also lower than that of *A. longipes* (Rana et al. 2015). Male and female varieties of *Borassus aethiopum* have densities between 0.26–0.86 g/cm^3 and 0.21–0.75 g/cm^3 from inner to outer position, respectively (Lego et al. 2018). Date palm stems (*Phoenix dactylifera* L.) were found to have wet and dry densities of 0.46 g/cm^3 and 0.69 g/cm^3, respectively (Rizanti et al. 2018). The density distribution of palm wood is contingent upon the number of FVB and parenchyma tissue (Ishiguri et al. 2007). The density distribution of Indonesian sugar palm wood is determined by the unique structure and content of the palm trunk, as well as its capacity to adjust to the tropical environment. While the core is typically not commercially used, the outer section is highly valued for its strength, durability, and versatility in industries such as construction and furniture manufacturing. Density variation can be linked to the quantity and arrangement of vascular bundles and the diameter and thickness of the cell walls within the bundles.

Vertical density also decreased from the bottom to the upper position, with a consistent pattern for each horizontal section, except at the bottom (Table 2). The variations may result from climate conditions during growth, geographical site, and tree age (Machado et al. 2014). Interestingly, the interaction between vertical and horizontal variations was highly significant, and the pattern was consistent for the same position.

Dimensional shrinkage

Generally, dimensional shrinkage increased from the bark to the pith, horizontally (Figure 4). Longui et al. (2014) reported the average value of volumetric shrinkage palm wood

Table 2. Average density from the top to bottom and surface to pith of an *A. longipes* stem.

Vertical direction	Density (g/cm^3)				
	Horizontal direction				
	4 cm	8 cm	12 cm	16 cm	20 cm
1 m	0.75 + 0.13 a	0.59 + 0.13 b	0.53 + 0.17 c	0.37 + 0.07 e	0.29 + 0.04 f
2 m	0.75 + 0.12 a	0.61 + 0.11 b	0.50 + 0.14 c	0.35 + 0.06 e	0.28 + 0.05 f
3 m	0.74 + 0.13 a	0.60 + 0.14 b	0.47 + 0.19 c	0.35 + 0.08 e	0.28 + 0.04 f
4 m	0.73 + 0.13 a	0.56 + 0.11 b	0.43 + 0.17 d	0.31 + 0.01 f	0.24+ 0.08 g
5 m	0.73 + 0.12 a	0.51 + 0.13 c	0.42 + 0.03 d	0.29 + 0.04 f	0.22 + 0.05 g
6 m	0.73 + 0.15 a	0.49 + 0.16 c	0.37 + 0.07 e	0.25 + 0.04 g	0.20 + 0.08 g
7 m	0.73 + 0.12 a	0.46 + 0.13 c	0.29 + 0.08 f	0.18 + 0.02 g	0.13 + 0.03 h

Note: Values represent means of five samples per location, while figures in parentheses represent one standard deviation. Values followed by same letters are not significantly different from each other by Duncan's multiple range test (α = 0.05).

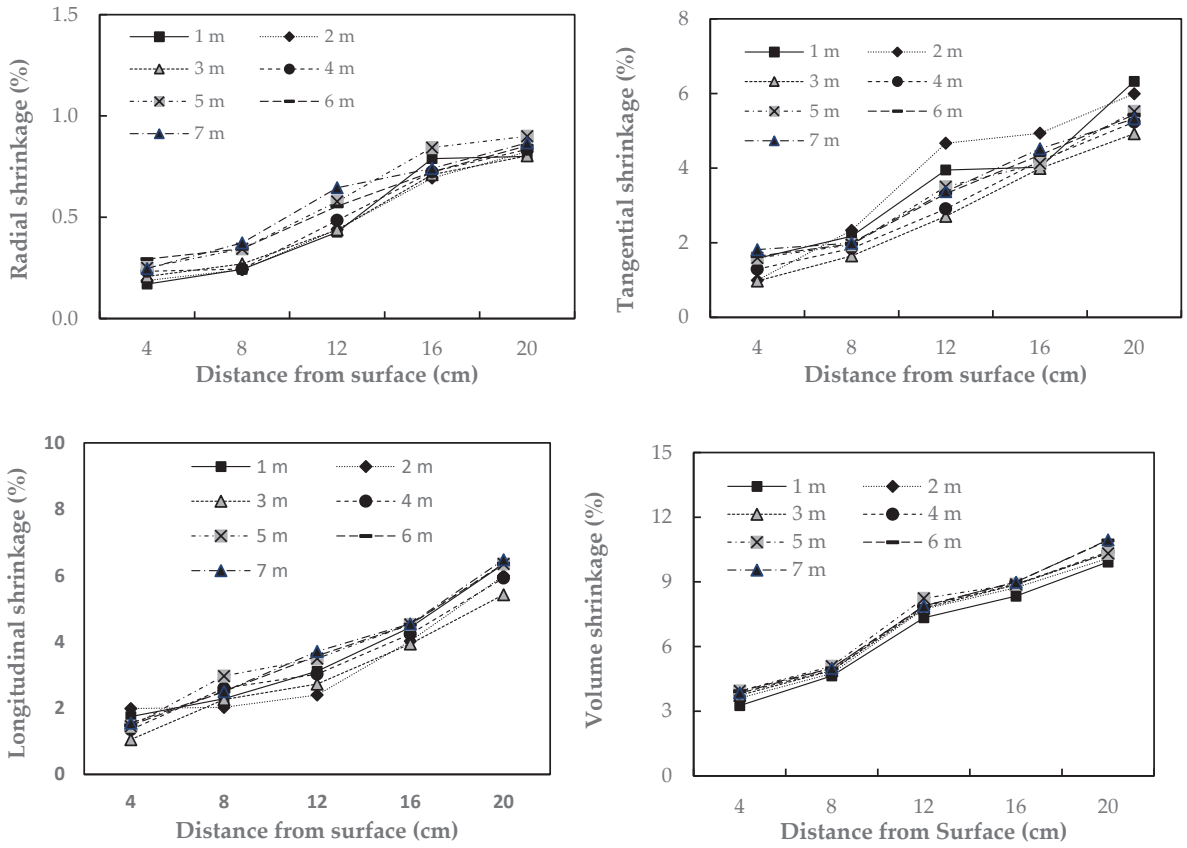

Figure 4. Dimensional shrinkage along the vertical and horizontal planes of an *A. longipes* trunk as the samples were dried from green to 12% moisture content.

decreased from the pith to the bark. These phenomena reflect the increased density *A. longipes* trunk from the bark to the pith (horizontally). Rahayu et al. (2021) reported that denser materials were more dimensionally stable. The shrinkage of wood is impacted by various factors, such as anisotropic shrinkage and alignment of the wood fibers in the trunk. In addition, the higher lignin content in the bark may have dimensional stability (Komisarz et al. 2023).

Longitudinal shrinkage was lower than tangential and radial shrinkage. This is consistent with the orientation of the fibers. Longitudinal shrinkage ranged from 0.17% to 0.87%, tangential shrinkage varied from 1.58% to 5.38%, radial shrinkage ranged from 1.74% to 6.48%, and volumetric shrinkage ranged from 3.26% to 10.95%. Shrinkage did not vary significantly from the bottom to the upper position, although shrinkage tended to increase with height. However, shrinkage tended to increase

significantly from the bark to the pith. Hartono et al. (2019) reported that volumetric shrinkage was lower, but the values were similar to those found by Nuryawan et al. (2017).

Modulus of ruptured and modulus of elasticity

The mechanical properties value of *A. longipes* at a distance greater than 12 cm from the bark was extremely low and is regarded as zero. The density value indicates that areas beyond 12 cm from the bark had lower density and exhibited twisting as a result of shrinkage. This occurred due to the presence of pores that facilitated water infiltration through capillary action, along with a significant amount of parenchyma tissue, that allowed water to be absorbed or evaporated quickly, depending on environmental conditions (Wulandari and Erwinsyah 2020). The trunk of *A. longipes* exhibits a distinct anatomical pattern regarding the horizontal orientation of the fibrovascular bundle, characterized by a decrease in FVB density as a one moves horizontally from the bark toward the pith. The reduced density of FVB will lead to a decline in strength in materials incorporating FVB tissue, such as that found in sugar palm trunks.

The outer layer of the trunk (close to the bark) exhibits a significantly higher density compared to the inner section influenced by the FVB density. The outer section is anatomically characterized by a higher composition of FVB with sclerenchyma fibers, in contrast to the parenchyma tissue that contains starch. This phenomenon results in the outer layer exhibiting greater strength than the inner layer. The values of MOR showed a notable decline as the distance from the ground increased, as well as with the distance inward from the surface at any specified height (Table 3). The observed values were generally greater than those established earlier for *A. Pinnata* (Nuryawan et al. 2017) and coconut wood (Rana et al. 2015).

In alignment with the MOR value pattern, the horizontal direction was exclusively assessed at a distance of 12 cm from the bark, with any measurement beyond this distance regarded as having value of zero (Table 4). There were no significant differences in MOE with distance from the ground nor in samples 4 and 8 cm from the outer edge; however, samples 12 cm inward did differ significantly between 1 to 3 m and 4 to 7 above ground.

A prior investigation involving *A. pinnata* indicated that the MOE value was consistently lower than that of *A. longipes* across all positions, with MOE values of *A. pinnata* ranging from 4.93 to 15.27 GPa (Nuryawan et al. 2017). When comparing the salacca palm frond, the MOE value is also lower than that of *A. longipes*: the measured value of MOE for salacca palm frond falls between 6 and 10 GPa (Hakim et al. 2021). Additionally, the MOE values comparison between *A. longipes* and coconut wood reveals distinct differences in values, with the measured values of MOE for coconut wood ranging from 1.8 to 14.03 GPa (Srivaro et al. 2018b).

In addition, the mechanical properties, including MOE and MOR, are also affected by the density of the *A. longipes* trunk. The analysis shown in Table 2, Table 3, and Table 4 illustrates the coherent relationship between density and mechanical properties. The section of the trunk exhibiting elevated density also demonstrated significant mechanical strength. The correlation between density and mechanical properties of *A. longipes* frond structure indicates that the high density of FVB tissue is associated with excellent mechanical properties compared to lower density material (Hakim et al. 2023).

3.4. Tensile and compression (parallel to grain) strength

The tensile strength and compression (parallel to grain) of *A. longipes* are summarized in Table 5 and 6. Similar to the

Table 3. MOR of *A. longipes* samples removed from selected heights above ground and distances inward from the surface.

Vertical direction	Horizontal direction (MPa)[a]		
	4 cm	8 cm	12 cm
1 m	143.49 ± 13.33 a	77.94 ± 2.69 d	19.73 ± 1.64 g
2 m	128.70 ± 15.23 a	66.98 ± 3.57 e	19.38 ± 2.75 g
3 m	122.83 ± 20.63 a	64.95 ± 5.38 e	18.01 ± 3.16 g
4 m	106.15 ± 11.48 b	63.07 ± 4.60 e	12.79 ± 3.30 h
5 m	100.32 ± 15.21 b	61.50 ± 1.78 f	12.11 ± 2.96 h
6 m	99.10 ± 17.89 b	60.77 + 1.72 f	11.25 + 1.76 h
7 m	96.79 ± 16.37 c	58.90 + 2.34 f	10.42 + 1.87 i

Note: Values represent means of five samples per location, while figures in parentheses represent one standard deviation. Values followed by same letters are not significantly different from each other by Duncan's multiple range test (α = 0.05).

Table 4. MOE of *A. longipes* removed from selected heights above ground and distances inward from the surface.

Vertical direction	Horizontal direction (GPa)[a]		
	4 cm	8 cm	12 cm
1 m	24.92 ± 1.51 a	12.98 ± 0.96 b	2.05 ± 0.52 c
2 m	22.78 ± 1.48 a	12.78 ± 0.96 b	1.59 ± 0.43 c
3 m	22.54 ± 1.32 a	12.65 ± 0.82 b	1.85 ± 0.50 c
4 m	21.31 ± 1.35 a	12.19 ± 0.96 b	0.81 ± 0.26 d
5 m	21.24 ± 1.10 a	11.77 ± 1.00 b	0.76 ± 0.21 d
6 m	17.53 ± 1.15 b	11.77 ± 1.07 b	0.73 ± 0.21 d
7 m	15.60 ± 1.33 b	9.94 ± 0.98 b	0.35 ± 0.11 d

Note: Values represent means of five samples per location, while figures in parentheses represent one standard deviation. Values followed by same letters are not significantly different from each other by Duncan's multiple range test (α = 0.05).

Table 5. Average value of variation direction (vertical and horizontal) for tensile strength of *A. longipes.*

Vertical direction	Horizontal direction (GPa)		
	4 cm	8 cm	12 cm
1 m	16.03 ± 2.29 a	8.98 ± 0.46 b	0.95 ± 0.32 c
2 m	16.01 ± 2.38 a	8.88 ± 0.46 b	0.89 ± 0.43 c
3 m	16.02 ± 2.22 a	8.52 ± 0.32 b	0.85 ± 0.20 c
4 m	16.01 ± 1.35 a	8.49 ± 0.36 b	0.78 ± 0.36 d
5 m	15.87 ± 1.10 a	8.48 ± 0.40 b	0.72 ± 0.41 d
6 m	15.77 ± 1.15 b	8.39 ± 0.37 b	0.68 ± 0.51 d
7 m	15.56 ± 1.33 b	8.38 ± 0.38 b	0.55 ± 0.21 d

Note: Values represent means of five samples per location, while figures in parentheses represent one standard deviation. Values followed by same letters are not significantly different from each other by Duncan's multiple range test (α = 0.05).

Table 6. Average value of variation direction (vertical and horizontal) for compression strength of *A. longipes.*

Vertical direction	Horizontal direction (MPa)		
	4 cm	8 cm	12 cm
1 m	6.14 + 1.19 a	1.16 + 0.52 b	0.92 + 0.12 c
2 m	5.89 + 1.48 a	1.15 + 0.46 b	0.92 + 0.23 c
3 m	5.97 + 1.32 a	1.11 + 0.42 b	0.57 + 0.15 c
4 m	5.57 + 1.35 a	1.06 + 0.56 b	0.56 + 0.16 d
5 m	5.42 + 1.10 a	1.06 + 0.39 b	0.57 + 0.11 d
6 m	5.13 + 1.15 b	1.03 + 0.47 b	0.53 + 0.18 d
7 m	5.13 + 1.33 b	1.01 + 0.48 b	0.53 + 0.13 d

Note: Values represent means of five samples per location, while figures in parentheses represent one standard deviation. Values followed by same letters are not significantly different from each other by Duncan's multiple range test (α = 0.05).

pattern for MOR and MOE, the horizontal direction was also only measured up to a distance of 12 cm from the bark, and more than 12 cm from the bark was considered to have a value of zero. Furthermore, the tensile strength and compression strength exhibited the highest value at 4 cm from the bark in the horizontal direction. The lowest value was observed at 12 cm from the bark in the horizontal direction. These phenomena are influenced by the density of the *A. longipes* trunk. Darwis et al. (2013) reported that the density influenced the mechanical properties of Palmae trunks. In addition, α-cellulose content in the bark observed in this study exceeded that of the pith of *A. longipes*. The α-cellulose serves as the primary component of the cell wall. Consequently, elevated α-cellulose content has been found to lead to thickened cell walls and enhanced mechanical properties (Ouyang and Wang 2022).

Relationships between density and mechanical properties

The correlations between density and MOR, along with MOE properties of *A. longipes,* are depicted in Figure 5a and 5b. The graph indicates a downward trend in the density, accompanied by a reduction in the MOR and MOE of the *A. longipes* trunk. The wood density of individual samples exhibits a moderate correlation with the mechanical properties of MOR and MOE. Consequently, it is feasible to accurately predict the strength of sugar palm trunks based on their density for individual samples, owing to this strong predictive capability.

The relationship between wood density and strength properties (MOR and MOE) is generally acknowledged, as density serves as an indicator of the relative quantity of solid cell wall

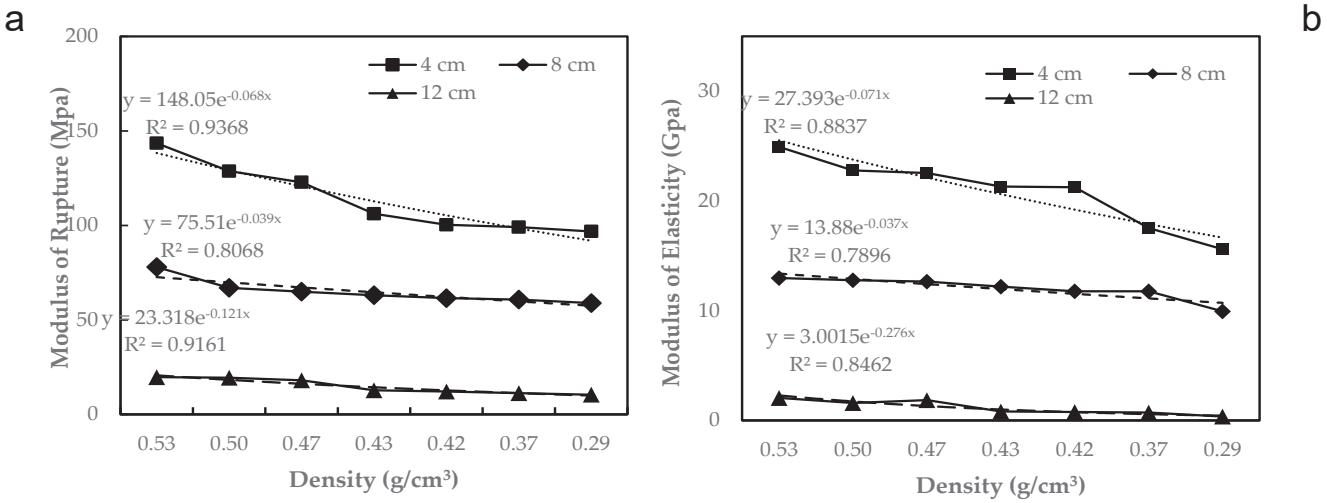

Figure 5. (a) Relationship between MOR and density; (b) Relationship between MOE and density.

(Wulandari and Erwinsyah 2020); however, the correlations are significantly influenced by the orientation, whether vertical or horizontal (Hakim et al. 2021; Srivaro et al. 2018a). In certain instance, the low-density correlations with mechanical properties were linked to the impact of the number of fibrovascular bundles (Hakim et al. 2022; Srivaro et al. 2018a). The reasoning is that as density increases, the number of FVBs also increases, which consequently affects the mechanical tests and leads to strong correlations when density is considered (Hakim et al., 2022). In addition, the previous discussion of chemical properties showed that the composition of cellulose and lignin from the outer to the inner (radial direction) *A. longipes* trunk also increased, as did MOE and MOR.

Gas chromatography–mass spectrometry analysis

The GC-MS analysis of the ethanol-benzene extract of *A. longipes* trunk resulted in the detection of 22 compounds that are presented in Table 7. Figure 6 shows the major compounds identified as hexadecanoic acid, vaccenic acid, 9-octadecenoic acid ethyl ester, tricosane, nonadecane, dodecane, 2,6,10-trimethyl-, and pentatriacontane. The components identified in this section of the trunk are nearly identical to those found in the bunch, which are mostly carboxylic acid-dominated (Hakim et al. 2024). Several linear acids such as hexadecanoic, heptadecanoic, and vaccenic were present, with significant percentage areas which are higher than the percentage areas of the acid components in the bunch (Hakim et al. 2024). The higher amount of acid in the *A. longipes* trunk may be influenced by the holocellulose content. As holocellulose decomposed between 250°C and 275°C, light oxygenates, acetic acid, furfural, and water are produced (Hamid et al., 2022). The degradation of lignin at 500°C–600°C produced phenolic compound, which was followed by esters and alkanes such as 3,7,11,15-tetramethyl-methyl ester, hexadecanoic acid ethyl ester, 9-octadecanoic acid ethyl ester, tricosane, tetracosane, nonadecane, and pentatriacontane. The esters compounds were

Table 7. The chemical compound of *A. longipes* trunk obtained in GC-MS analysis.

Peak	RT	Area (%)	Compound
1	4.898	-	1,2-Diphenylethan-1-ol
2	8.279	4.6	[Dodecanoyl(methyl)amino]Acetic Acid
3	9.79	-	Myristic Acid
4	11.22	97.98	n-Hexadecanoic acid
5	11.382	46.85	Hexadecanoic acid, ethyl ester
6	11.832	-	Heptadecanoic acid
7	12.42	84.77	cis-Vaccenic acid
8	12.57	100	9-Octadecenoic acid ethyl ester
9	12.743	27.26	Octadecanoic acid, ethyl ester
10	13.620	-	Heptadecane, 2,6,10,15-tetramethyl-
11	14.647	8.98	Tricosane
12	15.916	8.83	Nonadecane
13	17.531	11.63	Dodecane, 2,6,10-trimethyl-
14	18.523	-	1-(1-Ethoxyethoxy)-5-pentanol
15	19.596	19.73	Pentatriacontane
16	22.261	-	Tritriacontane
17	23.253	-	6,10,14-Hexadecatrienoic acid, 3,7,11,15-tetramethyl-, methyl ester, [R-(E,E)]-
18	25.71	-	Pentatriacontane
19	28.006	-	3-Acetoxypropyl trimethyl acetate
20	28.963	-	Pentatriacontane
21	31.005	-	Pentatriacontane
22	33.324	-	Tetracosane

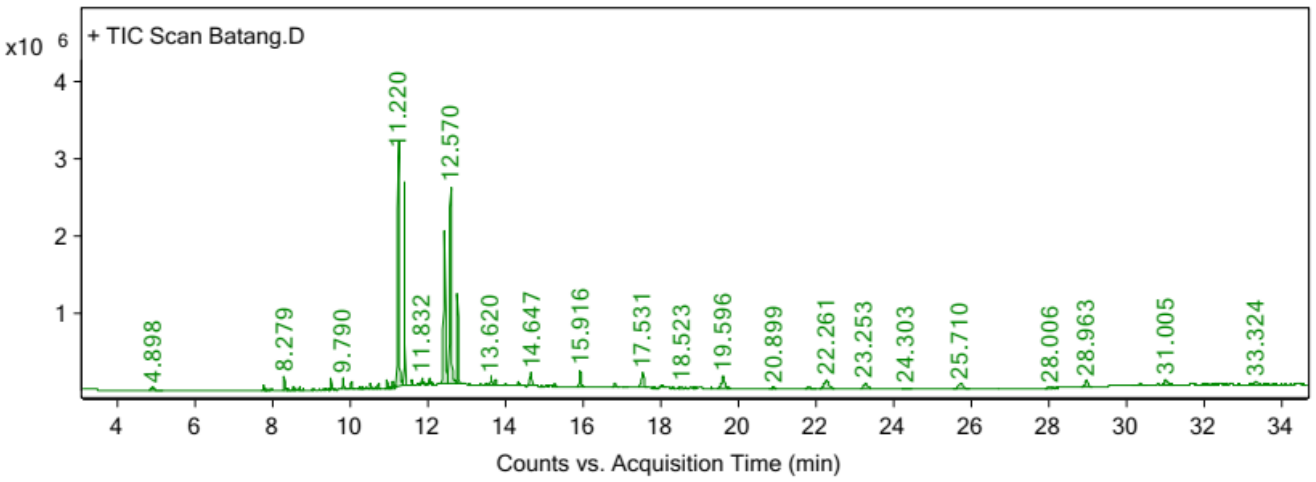

Figure 6. GC-MS chromatogram of *A. longipes* trunk.

also identified in *A. longipes* bunch and date palm biomass (Hamid et al. 2022), but the alkanes compound was unidentified in *A. longipes* bunch. This result could be due to lignin content because phenolic compounds are primarily produced through lignin decomposition, which involves cleaving ether linkages (β-O-4 and α-O-4 bonds) to generate the lignin monomer.

Fourier-transform infrared spectroscopy analysis.

Chemical studies of the functional groups found in the *A. longipes* trunk were studied using FTIR, as shown in Figure 7. A broad peak at around 3342 cm^{-1} due to stretching vibration of the O-H bond was observed in the sample, while peaks due to C-H bond stretching frequency were detected at 2851 cm^{-1}. These peaks were stronger for these samples because the cellulose content was higher, and the lignin and hemicellulose components of the raw biomass were lower. The broad absorption indicated the hydrophilic tendency of material, and it is attributed to the moisture content and hydroxyl functional group found in lignin, cellulose, and hemicellulose. The peaks at 1597 cm^{-1} indicated the presence of lignin; these are due to the stretching of C=C present in aromatic structure of lignin (Shaikh et al. 2021). Meanwhile, the peaks on 1219, 1329, and 1455 cm^{-1} could be indicated with the C-O carbonyl band in lignin and xylan units; these peaks are similar to that of *A. longipes* bunch. The peaks at 837–1162 cm^{-1} could correspond to both aliphatic and aromatic functional groups.

Thermogravimetry analysis

Thermal stability and weight loss behavior of *A. longipes* trunk was assessed by using TGA, and the result is shown in Figure 8. It is evident from Figure 8a that there was a significant weight loss at 402°C; temperature increased the mass loss of the biomass samples. Based on the graph in Figure 8b, the first phase had moisture evaporation at temperatures between 50–200°C, with a mass loss of 6.9%. This result was slightly different from that of Hakim et al. (2024), with the moisture evaporation leading to mass loss of 9.9%. The next phase was degradation of hemicellulose at around 250°C, and complete degradation at 402°C, with mass loss of 18%, reflecting carbohydrate losses loss. The *A. longipes* trunk thermal stability was illustrated by the DTG curves shown in Figure 8c. The maximum mass loss rate was at 290°C with a value of 1.08 mg/min. This result is supported by Werner et al. (2014), who found that polysaccharide decomposition occurs at a temperature range of 200–380°C, with xylan in particular experiencing a maximum mass loss rate at lower temperatures of 243°C and 292°C. However, this differed from Hakim et al. (2024), who reported that peak decomposition occurred at average temperature of 327°C (Figure 8d). According to Poletto et al. (2010), temperatures between 210°C and 300°C may be linked to the gradual breakdown of lignin and the breakdown of hemicellulose. Random cleavage of the cellulose's glycosidic bond

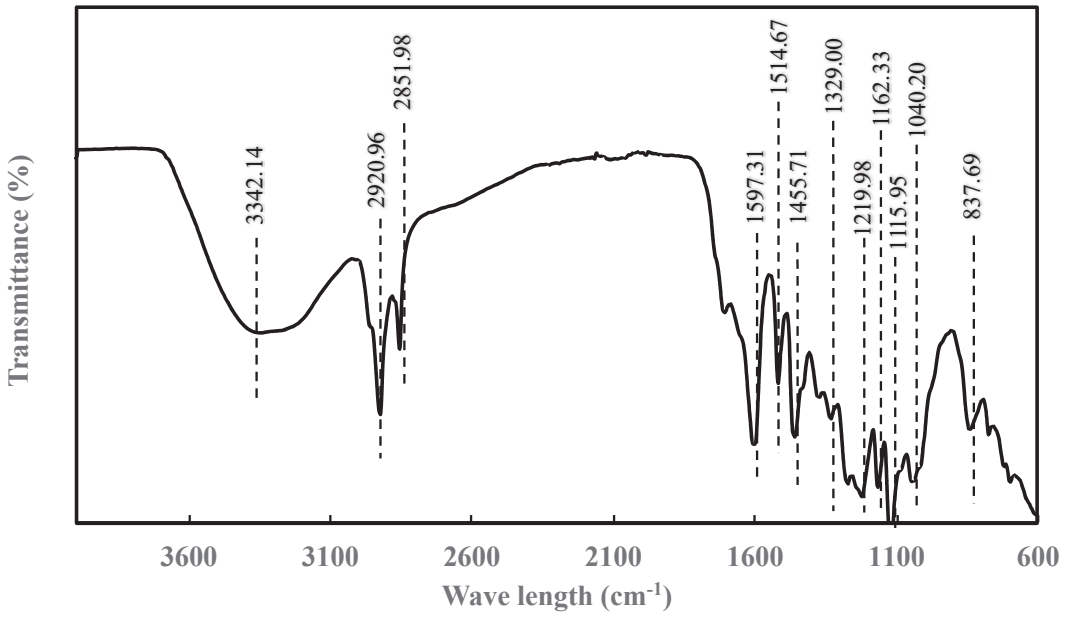

Figure 7. FTIR spectra of *A. longipes* trunk.

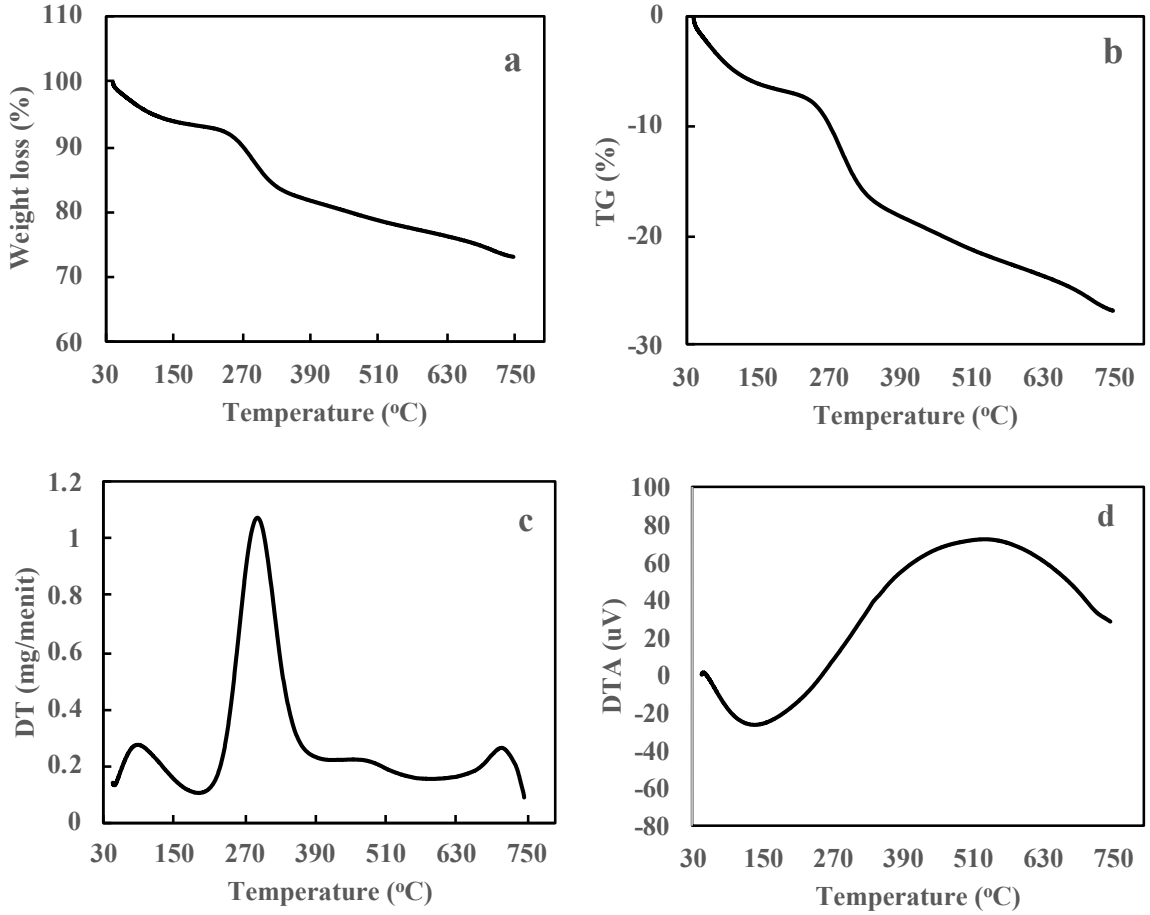

Figure 8. Thermogravimetric curve of *A. longipes* trunk. (a). Weight loss; (b). Thermo- stability; (c). Differential thermal stability; (d). Differential thermal analysis.

occurs between 275°C and 350°C, while lignin decomposes between 250°C and 500°C.

Variability of properties and utilization

Although *A. longipes* is a palm species that exhibits significant variability due to site and climatic conditions, it demonstrates high variability within individual trunks. This study examines the fundamental characteristics in both the vertical and horizontal directions. Differences in the variation of properties within the trunk of *A. longipes* are a significant factor contributing to variation in its basic characteristics. The effect of trunk position on *A. longipes* should be considered when selecting the appropriate end use. Horizontally, the potential for using *A. longipes* as construction wood would be more suitable if limited to the peripheral section, approximately 3–4 cm thick, from the bark. Material more than 4 cm from the bark is no longer suitable for use as building or construction timber under heavy loads. The influence of individual plants on various wood properties should be considered in the selection process and for improving wood quality.

Regarding within-trunk variation, horizontal variation was the most significant for all properties of the sugar palm trunk, highlighting the importance of *A. longipes* trunk characteristics in determining suitable uses. These variations follow a trend of increasing trunk quality from the pith to the outer peripheral zones (bark), which is related to chemical content and density. In this study, the horizontal position at 4 cm from the bark exhibited favorable properties (density, MOE, and MOR), with values gradually decreasing toward the pith. However, vertical variation within the trunk showed minimal range, making it less of an obstacle in quality selection and advantageous for utilizing *A. longipes* trunks along their full length, from bottom to top. GC-MS analysis revealed that the *A. longipes* trunk contains several compound categories, such as acids, esters, and alkanes. One of the acidic compounds,

vaccenic acid, may have further utility as it has been identified as a prominent compound that has antimicrobial properties.

Conclusions

The *A. longipes* palm from Sumatera, Indonesia, exhibited high-quality wood-like properties in the outermost 4 cm of its trunk diameter. The stems exhibited moderate to low density from the outermost to the innermost trunk position, which was associated with increased flexural properties closer to the outer edges. No significant differences were observed with distance above ground, and within-trunk heterogeneity was minimal. The outermost regions of the *A. longipes* trunk have potential as a substitute for industrial wood. The predominant chemicals found in the stems of *A. longipes* included n-hexadecanoic acid, 9-octadecenoic acid ethyl ester, and vaccenic acid, which are common fatty acids derived from palm plants and have potential antibacterial properties. Thermal analysis indicated that *A. longipes* stems undergo thermal degradation at temperatures up to 402°C, resulting in an 18% weight loss.

Author Contributions: All authors have contributed equally.

Funding: This research was funded by World Class University (WCU) Grant No. 40/UN5. 2.3.1/PPM/KP-WCU/2022, the Indonesian Endowment Fund for Education (LPDP), Ministry of Finance, Republic of Indonesia.

Data Availability Statement: The data presented in this study are available on request from the corresponding author.

Acknowledgments: The authors are grateful to Universitas Sumatera Utara for funding this research through the World Class University (WCU) grant, the Indonesian Endowment Fund for Education (LPDP), Ministry of Finance, Republic of Indonesia. The authors would also like acknowledge Laboratory of Forest Product Technology, Faculty of Forestry, Universitas Sumatera Utara for providing equipment to carry out the experiment.

Conflicts of Interest: The authors declare no conflict of interest.

References

ASTM (2021) D 1102. Standard test method for ash in wood. American Society for Testing and Materials, West Conshohocken, PA. USA. https://store.astm.org/d1102-84r21.html

ASTM (2001) D 1103. Standard test method for alpha cellulose in wood. American Society for Testing and Materials, West Conshohocken, PA. USA. https://www.document-center.com/standards/show/ASTM-D1103

ASTM (1978) D 1104. Standard test method for holocellulose in wood. American Society for Testing and Materials, West Conshohocken, PA. USA. https://www.document-center.com/standards/show/ASTM-D1104

ASTM (2021) D 1106. Standard test methods for acid insoluble lignin in wood. American Society for Testing and Materials, West Conshohocken, PA. USA. https://store.astm.org/d1106-21.html

Azhar I, Risnasari I, Muhdi, Srena MF, Riswan (2019) The Utilization of Sugar Palm (*Arenga pinnata*) by the People Around Batang Gadis Nasional Park Area. IOP Conf Ser: Earth Env Sci 305 012016:1–7. https://doi.org/10.1088/1755-1315/305/1/012016.

BPS (2021) Statistik Perusahaan Perkebunan Provinsi Sumatera Utara 2020. Badan Pusat Statistik Provinsi Sumatera Utara. Indonesia. https://sumut.bps.go.id/id/publication/2021/12/23/6b4fca56257b3152776ef37f/statistik-perusahaan-perkebunan-provinsi-sumatera-utara-2020.html

British Standard (1957) BS 373: Methods of testing small clear specimens of timber. https://www.en-standard.eu/bs-373-1957-methods-of-testing-small-clear-specimens-of-timber/

Darwis A, Nurrochmat DR, Massijaya Y, Nugroho N, Alamsyah EM, Bahtiar ET, Safe'i R (2013) Vascular bundle distribution effect on density and mechanical properties of oil palm trunk. Asian J Plant Sci 12(5):208–213. https://doi.org/10.3923/ajps.2013.208.213

Fadhilla S, Hakim L, Agustian A, Lubis YS, Siregar AW (2023) The diversity of utilizations, tapping flow discharge, and conservation of sugar palm (*Arenga longipes* Mogea) cultivated in Langkat, North Sumatra, Indonesia. Biodiversitas 24(1):122–132. https://doi.org/10.13057/BIODIV/D240116

Gunawan R, Ramadhan UG, Iskandar J, Partasasmita R (2018) Local knowledge of utilization and management of sugar palm (*Arenga pinnata*) among Cipanggulaan People of Karyamukti, Cianjur (West Java, Indonesia). Biodiversitas 19(1):93–105. https://doi.org/10.13057/biodiv/d190115

Hakim L, Batubara R, Manurung H, Silitonga VW (2023) Longitudinal and radial variability of anatomical properties, fiber morphology, and mechanical properties of fibrovascular bundle from Indonesian *Arenga longipes* Mogea sp. nov frond. J Nat Fibers 20(2):1–16. https://doi.org/10.1080/15440478.2023.2224978

Hakim L, Iswanto AH, Herawati E, Batubara R, Lubis YS, Aini EN (2024). Characterization of Indonesian sugar palm bunch (*Arenga longipes* Mogea) properties for various utilization purposes. Forests 15(2):1–15. https://doi.org/10.3390/f15020239

Hakim L, Widyorini R, Nugroho WD, Prayitno TA (2021) Radial variability of fibrovascular bundle properties of salacca (*Salacca zalacca*) fronds cultivated on turi agrotourism in Yogyakarta, Indonesia. Biodiversitas *22*(8):3594–3603. https://doi.org/10.13057/biodiv/d220861

Hakim L, Widyorini R, Nugroho WD, Prayitno TA (2022) Effect of vascular tissue on mechanical properties of fibrovascular bundles of *Salacca Sumatrana* Becc. fronds. J Nat Fibers 19(14):1–14. https://doi.org/10.1080/15440478.2021.1982824

Hamid FA, Zainal NH, Othman NEA, Ismail F, Wahab NA, Aziz AA (2022) Characterization of palm pyroligneous acid and its effectiveness as antifungal agent for oil palm trunk. J Oil Palm Research 34(4):678–685. https://doi.org/10.21894/jopr.2022.0007

Hartono R, Muhdi, Nainggolan JP (2019) The physical properties and the extractive content of sugar palm stem (*Arenga pinnata*). J Sylva Indonesiana 2(1): 37–46. https://doi.org/10.32734/jsi.v2i1.813

Haryoso A, Zuhud EAM, Hikmat A, Sunkar A, Darusman D (2020) Ethnobotany of sugar palm (*Arenga pinnata*) in the sasak community, Kekait village, West Nusa Tenggara, Indonesia. Biodiversitas 21(1):117–128. https://doi.org/10.13057/biodiv/d210116

Imraan M, Ilyas RA, Norfarhana AS, Bangar SP, Knight VF, Norrrahim MNF (2023) Sugar palm (*Arenga pinnata*) fibers: new emerging natural fibre and its relevant properties, treatments and potential applications. J Mater Res Technol 24 (May-Jun):4551–4572. https://doi.org/10.1016/j.jmrt.2023.04.056

Ishiguri F, Eizawa J, Saito Y, Iizuka K, Yokota S, Priadi D, Sumiasri N, Yoshizawa N (2007) Variation in the wood properties of *Paraserianthes falcataria* planted in Indonesia. IAWA J 28(3):339–348. https://doi.org/10.1163/22941932-90001645

Johnson DV (1992) Palm utilization and management in Asia: examples for the neotropics. Bulletin de l'Institut Français d'études Andines 21(2): 727–740. https://doi.org/10.3406/bifea.1992.1084

Komisarz K, Majka TM, Pielichowski K (2023) Chemical and physical modification of lignin for green polymeric composite materials. Materials 16(1):1–40. https://doi.org/10.3390/ma16010016

Lego K, Sharma C, Sharma M (2018) Axial variation of wood density in *Pinus merkusii* Jungh. & de Vriese. J Tree Sci, *37*(1):1–10. https://doi.org/10.5958/2455-7129.2018.00001.8

Longui E L, Romeiro D, Pfleger P, Lima IL, Silva FG, Garcia JN, Bortoletto G, Neto AOLF, Florsheim SMB (2014) Radial variation of anatomical features, physicomechanical properties and chemical constituents and their potential influence on the wood quality of 45-year-old *Eucalyptus propinqua*. Aust For *77*(2):78–85. https://doi.org/10.1080/00049158.2014.905739

Lovestead TM, Urness KN (2019) Gas chromatography-mass spectrometry (GC−MS). *ASM International Handbook*. National Institute of Standards and Technology. https://tsapps.nist.gov/publication/get_pdf.cfm?pub_id=926655.

Machado JS, Louzada JL, Santos AJA, Nunes L, Anjos O, Rodrigues J, Simões RMS, Pereira H (2014) Variation of wood density and mechanical properties of blackwood (*Acacia melanoxylon* R. Br.). Mater Design 56(April):975–980. https://doi.org/10.1016/j.matdes.2013.12.016

Mogea JP (2004) Four new species of Arenga (Palmae) from Indonesia. Reinwardtia, 12(2):181–189. https://archive.org/details/reinwardtia-12-181-189.

Mogea MJ, Seibert B, Smits W (1991) Multipurpose palms: the sugar palm (*Arenga pinnata*). Agroforest Syst 13:111–129. https://link.springer.com/article/10.1007/BF00140236.

Muda M, Muda NA, Awal A (2024) Sugar palm (*Arenga pinnata* Wurmb Merr.): Its potential, limitation, and impact on socio-economic development of rural communities in Malaysia. J Nat Fibre Poly Comp *3*(1)5:1–8. https://239ec624-ab30-45de-8e11-0d1c08b34d22.filesusr.com/ugd/391d16_4677fbc829f741e4857ad38be2195750.pdf.

Nirawati, Restu M, Kuswinanti T, Musa Y, Paembonan SA, Millang S, Syahidah, Larekeng SH (2020) Morphological characteristics of *Arenga pinnata* Merr. from Maros and Sinjai Provenances in South Sulawesi, Indonesia, and its relationship with brix content. IOP Conf Ser: Earth Env Sci 486 012080:1–5. https://doi.org/10.1088/1755-1315/486/1/012080.

Nuryawan A, Tarigan A, Hakim L (2017). The feasibility of sugar palm (*Arenga pinnata*) trunk for raw material of parquet (wood flooring). IOP Conf Ser: Mater Sci Eng 180 012017:1–7. https://doi.org/10.1088/1757-899X/180/1/012017.

Ouyang F, Wang W (2022) Effect of thermo-hydro-mechanical treatment on mechanical properties of wood cellulose: A molecular dynamics simulation. Forests 13(6)903:1–11. https://doi.org/10.3390/f13060903.

Pillai AR, Riyas CT, Sabu KK (2020) A review on the unexplored and underutilized Arenga species in India. Current Botany 11:226–232. https://doi.org/10.25081/cb.2020.v11.6252

Poletto M, Dettenborn J, Pistor V, Zeni M, Zattera J (2010) Materials produced from plant biomass. Part I: Evaluation of thermal stability and pyrolysis of wood. Mater Res 13 (3, Sept):375–379. https://doi.org/10.1590/S1516-14392010000300016

Rahayu I, Dirna FC, Maddu A, Darmawan W, Nandika D, Prihatini E (2021) Dimensional stability of treated sengon wood by nano-silica of betung bamboo leaves. Forests 12(11)1581:1–9. https://doi.org/10.3390/f12111581

Rana M, Das A, Ashaduzzaman M (2015) Physical and mechanical properties of coconut palm (*Cocos nucifera*) stem. Bangladesh J Sci Industr Res 50(1):39–46. https://doi.org/10.3329/bjsir.v50i1.23808.

Rizanti DE, Darmawan W, George B, Merlin A, Dumarcay S, Chapuis H, Gérardin C, Gelhaye E, Raharivelomanana P, Sari RK, Syafii W, Mohamed R, Gerardin P (2018) Comparison of teak wood properties according to forest management: short versus long rotation. Annals Forest Sci, 75(39):75–89. https://doi.org/10.1007/s13595-018-0716-8

Sahari J, Sapuan SM, Ismarrubie ZN, Rahman MZA (2012) Physical and chemical properties of different morphological parts of sugar palm fibres. Fibres Text East Eur 91(2): 21–24. http://www.fibtex.lodz.pl/article682.html.

Shaikh HM, Anis A, Poulose AM, Al-Zahrani SM, Madhar NA, Alhamidi A, Alam MA (2021) Isolation and characterization of alpha and nanocrystalline cellulose from date palm (*Phoenix dactylifera* l.) trunk mesh. Polymers 13(11)1893:1–14. https://doi.org/10.3390/polym13111893.

Srivaro S, Matan N, Lam F (2018a) Property gradients in oil palm trunk (*Elaeis guineensis*). J Wood Sci 64:709–719. https://doi.org/10.1007/s10086-018-1750-8.

Srivaro S, Rattanarat J, Noothong P (2018b) Comparison of the anatomical characteristics and physical and mechanical properties of oil palm and bamboo trunks. J Wood Sci, 64:186–192. https://doi.org/10.1007/s10086-017-1687-3.

Srivaro S, Tomad J, Shi J, Cai J (2020) Characterization of coconut (*Cocos nucifera*) trunk's properties and evaluation of its suitability to be used as raw material for cross laminated timber production. Cons Build Mater 254:1–14. https://doi.org/10.1016/j.conbuildmat.2020.119291.

Takoumbe C, Tiaya EM, Ndapeu D, Mejouyo PWH, Wagang CVK, Njeugna E, Bistac S (2023) Selected physical and mechanical properties of the oil palm pseudo-trunk: Case of the Tenera variety from Cameroon. Results in Mater 17(March):1–8. https://doi.org/10.1016/j.rinma.2022.100354

Werner K, Pommer L, Broström M (2014) Thermal decomposition of hemicelluloses. J Analytical Appl Pyrolysis, 110(1):130–137. https://doi.org/10.1016/j.jaap.2014.08.013

Wulandari A, Erwinsyah E (2020) Distribution of vascular bundles and physical properties analysis of variety DxP oil palm trunk based on various zones and trunk heights. Jurnal Penelitian Kelapa Sawit 28(1):1–14 https://jurnalkelapasawit.iopri.org/index.php/jpks/article/view/93